Animal Reproduction Science 211 (2019) 106225

Contents lists available at ScienceDirect

Animal Reproduction Science

journal homepage: www.elsevier.com/locate/anireprosci

Abundances of autophagy-related protein LC3B in granulosa cells, cumulus cells, and oocytes during atresia of pig antral follicles

Luisa Gioia[a,*], Claudio Festuccia[b], Alessandro Colapietro[b], Alessia Gloria[c], Alberto Contri[a], Luca Valbonetti[a]

[a] Faculty of Bioscience and Technology for Food, Agriculture and Environment, University of Teramo, Via R. Balzarini 1, 64100, Teramo, Italy
[b] Department of Biotechnological and Applied Clinical Sciences, University of L'Aquila, Via Vetoio, Coppito 2, 67100, L'Aquila, Italy
[c] Faculty of Veterinary Medicine, University of Teramo, Loc. Piano D'Accio, 64100, Teramo, Italy

ARTICLE INFO

Keywords:
LC3B
Autophagy
Atresia
Pig
Granulosa cells
Cumulus cells

ABSTRACT

In mammals, apoptosis has been accepted as the type of programmed cell death (PCD) that occurs in ovarian follicles undergoing atresia. Results of recent studies, however, indicate autophagy may be an alternative mechanism involved in follicle depletion through independent or tandem actions with apoptosis. Western blotting and immunofluorescence procedures were used in the present study to investigate the abundances of LC3B protein in freshly collected granulosa cells (GCs), cumulus cells (CCs), and oocytes to evaluate whether autophagy is an important process of antral follicle atresia in sexually mature sows. Furthermore, apoptosis was analyzed using annexin V and TUNEL assays in the same cellular cohorts to evaluate the correlation between the two processes. Immunostaining results indicate autophagy was induced in the majority of GCs, CCs, and oocytes from early and advanced stage atretic follicles. The quantitative results of western blot analysis indicate there is a progressive increase ($P < 0.05$) in abundance of autophagy-related protein (LC3B-II) in these cells compared with cells in non-atretic follicles. Furthermore, there is confirmation that apoptosis occurs in the GCs of atretic follicles, thus indicating that in pigs apoptosis and autophagy are processes in GCs that regulate PCD and as a consequence antral follicle depletion. There was a greater abundance of LC3B-II in CCs and oocytes of atretic follicles, while apoptosis was not detected. It, therefore, is suggested that in these cells the two processes function independently, with autophagy having a cytoprotective rather than PCD mechanism of action.

1. Introduction

The ovary is a dynamic organ that eliminates excessive and defective germ cells to ensure the ovulation of oocytes with the capacity for fertilization and embryo development. To ensure this aim, more than 99% of follicles in mammalian ovaries undergo atresia and are selectively eliminated during the reproductive lifespan of mammals (Manabe et al., 2004; Matsuda et al., 2012). Follicular atresia involves mechanisms of programmed cell death (PCD), with apoptosis being the primary apoptotic regulatory mechanism (Kaipia and Hsueh, 1997) and GCs being the cells affected to the greatest extent (Regan et al., 2018).

The pattern of apoptosis is different among species. Although apoptosis occurs in GCs during follicular atresia both in rodents and in pigs (Byskov, 1974; Morita and Tilly, 1999; Manabe et al., 2004; Lin and Rui, 2010; Escobar Sánchez et al., 2012;Meng et al.,

* Corresponding author.
E-mail address: lgioia@unite.it (L. Gioia).

https://doi.org/10.1016/j.anireprosci.2019.106225
Received 3 August 2019; Received in revised form 15 October 2019; Accepted 26 October 2019
Available online 04 November 2019
0378-4320/

2018), in pigs apoptosis does not occur in CCs and oocytes at the early stage of atresia, unlike what occurs in rodents (Manabe et al., 1997).

Interestingly, results of recent studies indicate there is an alternative mechanism of PCD, autophagy, which may be an important process contributing to ovarian follicle depletion, functioning independently or in tandem with apoptosis in processes of PCD (Ortiz et al., 2006; Morais et al., 2012; Escobar et al., 2013; Yadav et al., 2018). Autophagy has been determined to be a process involved in GC death and follicular atresia in humans (Duerrschmidt et al., 2006; Serke et al., 2009; Vilser et al., 2010) and rats (Choi et al., 2010, 2014), while reports are still scarce for other mammalian species (Ryter et al., 2014). In particular, for pigs, the occurrence of autophagy in GCs has been mainly documented *in vitro* when there is gonadotropin stimulation or when there are stressed conditions (Gao et al., 2016; Hale et al., 2017). Kim et al. (2013) compared the *in vivo* expression of the cloned MAP1LC3A gene in GCs from normal and miniature pigs; however, there was no indication that the process of atresia was studied, and the investigation was not performed in CCs or in oocytes.

The main objective of the present study, therefore, was to evaluate, for the first time, the occurrence of autophagy *in vivo* in GCs of pigs, as well as in oocytes and the surrounding CCs, during follicular atresia at the antral stage by analyzing the expression and subcellular distribution of the LC3B protein, which is a reliable and widely used autophagic marker (Klionsky and Schulman, 2014). We also examined the incidence of apoptosis in the same cell populations and its correlation with autophagy to contribute to the knowledge of the molecular mechanisms involved in the PCD of GCs in swine.

2. Materials and methods

2.1. Reagents

All reagents were procured from Sigma Aldrich (St. Louis, MO, USA), unless otherwise stated.

2.2. Ovarian follicle selection and classification

Ovaries from sexually mature Large White sows collected immediately after slaughter were transported to the laboratory and processed using the previously validated protocols (Mattioli et al., 2003; Gioia et al., 2005). Based on the follicular health status, follicles were classified into three groups (Fig. 1A) according to previously validated morphological criteria (Meineke et al., 1982; Lin and Rui, 2010; Wang et al., 2012). Healthy follicles were well-vascularized, translucent, and without any debris floating in the clear follicular fluid; early atretic follicles (ATR +) appeared quite opalescent, with little vascularization, and some floating debris inside; advanced atretic follicles (ATR + + +) were opaque, with very little or no vascularization, and these follicles had a large amount of debris floating in the follicular fluid. For the present study, a total of 200 follicles and the cumulus-oocyte complexes/group were collected to perform the apoptosis and autophagy analyses that are subsequently described in this manuscript.

2.3. GC, CC, and oocytes recovery

After follicle classification, GCs, CCs, and oocytes from each of the three groups were collected and pooled as subsequently described in this manuscript. An incision was made in each follicle and there was eversion of the follicle using a dissection microscope, and the cumulus-oocyte complex was then isolated and collected. The follicular fluid was aspirated, and the granulosa cell layer was gently scraped into D-PBS. The GCs collected from both the follicular fluid and follicular wall were pooled and manually dissociated using a 1-mL syringe with a 23 G needle to achieve cell separation (Kim et al., 2013) and number of cells were then counted using a haemocytometer to determine the GC density.

Pools of CCs were collected from the same follicles from which GCs were collected by gently pipetting the cumulus-oocyte complexes in D-PBS and then using the same procedure as previously describe in this manuscript to achieve CC dissociation. The cumulus-free oocytes were removed and pooled for each group. For each condition (healthy, ATR + , ATR + + +), the pools of GCs, CCs, and oocytes were divided into two aliquots, which were then used to evaluate apoptosis or autophagy (see Supplementary Fig. I).

2.4. Evaluation of apoptosis

2.4.1. Annexin V-FITC/PI staining to detect early apoptosis in GCs, CCs, and oocytes

An annexin V assay (InVitrogen, Carlsbad, CA, USA) was conducted on fresh GCs, CCs, and oocytes, within 1 h after collection from healthy or atretic antral follicles, to evaluate early apoptosis (Anchordoquy et al., 2014). Briefly, GC suspensions were filtered through a 30 μm nylon mesh filter to eliminate any remaining aggregated cells and washed twice in ice-cold PBS by centrifugation at 300 × *g* for 5 min at 4 °C. The pellets were re-suspended in 100 μL of annexin V binding buffer solution, processed according to the double staining procedure proposed by Vermes et al. (1995), and there was immediate analysis using a MoFlo Astrios flow cytometer (Beckman Coulter, San Jose, CA, USA) equipped with an ion laser with a 488 nm wavelength. For all evaluations, a gate was created with the side scatter and forward scatter plot so that there was only evaluations of GCs. Events were acquired using FL1 (513/26 nm) for annexin V and FL3 (620/29 nm) for PI. Annexin V-positive events were considered to be indicative of apoptotic cells, while those with PI positivity or with annexin V/PI co-positivity were considered to be necrotic cells. With these analyses, which were performed in triplicate, the flow rate was adjusted to 150–250 events/sec, and acquisition was stopped at 10,000 events.

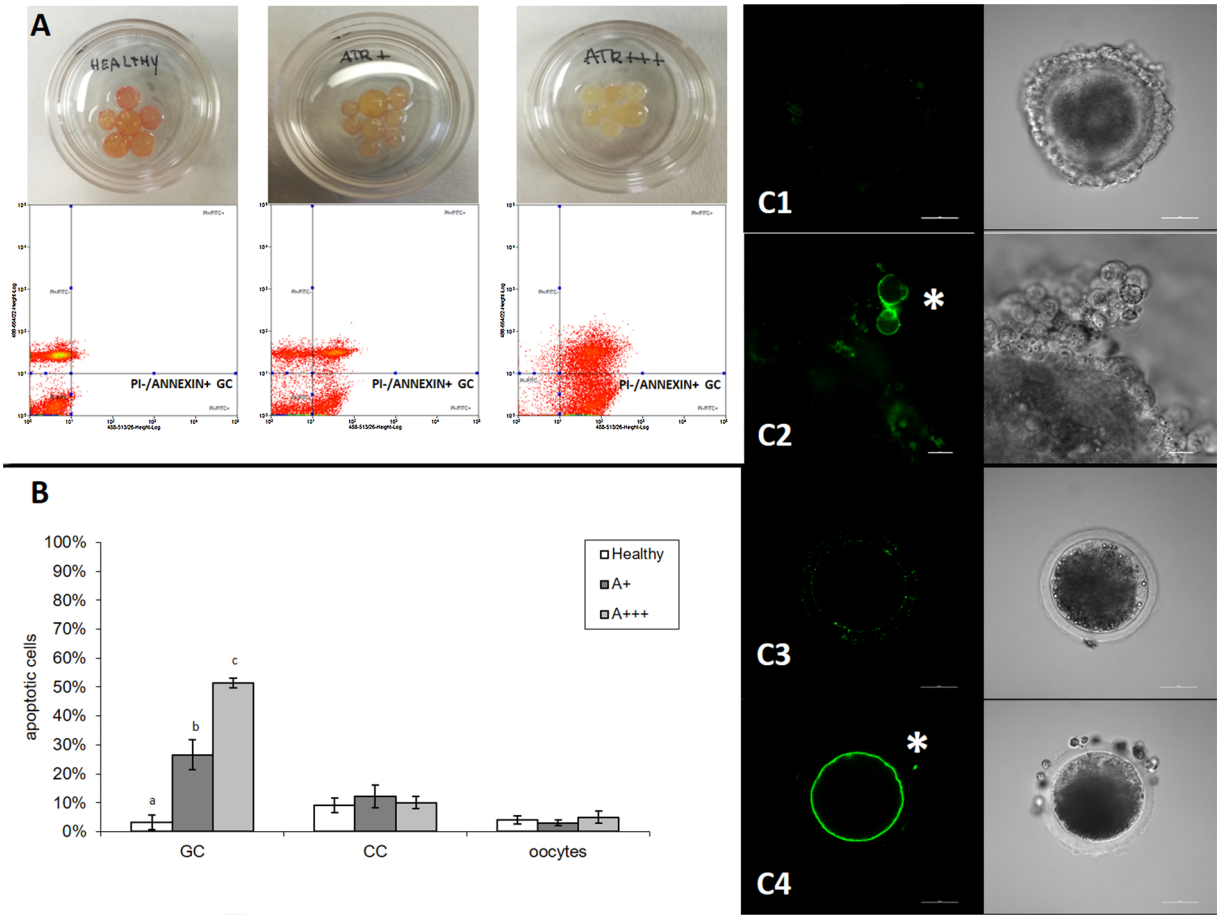

Fig. 1. Analysis of early apoptosis in granulosa cells (GCs), cumulus cells (CCs), and oocytes of sows collected from healthy or atretic follicles. (A) Representative flow cytometry plots of early apoptosis determined using annexin V-FITC/PI staining in GCs collected from healthy, early atretic (ATR+), and advanced atretic (ATR+++) antral follicles; Early apoptotic (PI-/annexin+) GCs are shown in the lower right quadrant; (B) Graph illustrating the percentages of apoptotic GCs, CCs, and oocytes detected in the different follicle groups (three independent experiments); Different superscript letters indicate differences ($P < 0.05$); (C) Representative confocal microscopy images of CCs and cumulus-free oocytes evaluated using annexin V/PI staining; Asterisks represent early apoptotic CCs (C2) and oocytes (C4), with plasma membranes having a green color due to phosphatidylserine externalization; healthy CCs and oocytes without any fluorescence are shown in C1 and C3, respectively; Scale bars in C1, C3, C4: 50 μm; scale bar in C2: 10 μm

The annexin V/PI assay was also used to evaluate early apoptosis in CCs and in cumulus-free oocytes taken from healthy, ATR+, and ATR+++ follicles. After staining, the exposure of phosphatidylserine on the outer portion of the plasma membrane was evaluated using confocal microscopy. Three independent analyses were conducted, with at least 200 CCs and 10 oocytes being analyzed per group.

2.4.2. TUNEL assay in GCs, CCs, and oocytes

Late apoptosis was detected using a TUNEL assay in each group of GCs, CCs, and oocytes using the ApopTag fluorescein *in situ* apoptosis detection kit (Millipore, Merck, Darmstadt, Germany) by conducting the previously described procedures of Mohn et al. (2015). At the end of the protocol, the GCs were analyzed using flow cytometry. For all evaluations, a gate was created with the side scatter and forward scatter plot to consider only GCs, and a further gate was created for the PI-positive events. Events were acquired with FL1 (513/26 nm) for TUNEL and FL3 (620/29 nm) for PI, and those with green fluorescence on FL1 were considered to have DNA fragmentation. The flow rate was adjusted to 150–250 events/sec, and the acquisitions were stopped after 5000 events.

The DNA fragmentation was also evaluated in oocytes and CCs using a TUNEL assay adapted for these cells. At the end of the protocol, nuclei were counter-stained with PI (20 μM), and oocytes and cumulus-oocyte complexes were mounted on slides using ProLong Gold antifade reagent (InVitrogen) and were individually analyzed using a confocal microscopy to evaluate the percentage of TUNEL-positive cells. Oocytes pre-treated with DNase I served as a positive control for the assay. For each group, three independent analyses were conducted for GCs, and at least 200 CCs and 10 oocytes were evaluated using these procedures.

2.5. Evaluation of autophagy

2.5.1. Western blotting analysis of LC3B abundance in GCs, CCs, and oocytes

For each condition, pools of freshly collected GCs (2×10^6 cells/mL) and pools of 100 isolated oocytes and of the corresponding CCs were used. These cells were collected using procedures previously described in this manuscript, washed twice in D-PBS, and stored at −20 °C until western blotting analysis. For a positive control (rapamycin-treated cells), a group of cells was treated for 1 h with 1 μM rapamycin solution (Abcam, Cambridge, UK; ab120224) prior to fixation to chemically induce autophagy.

The cells were analysed to examine the amount of LC3B-I protein converted to LC3B-II, which is an index of autophagic induction. For the analyses, cells were lysed, the total protein concentration was biochemically determined, and a similar amount of protein was loaded for SDS-PAGE electrophoresis, followed by transfer to a nitrocellulose membrane, in accordance with the Bio-Rad protocol. The nitrocellulose membranes were exposed to primary antibodies against LC3B (1:100; Abcam, Cambridge, UK; ab48394) and GAPDH (diluted 1:1000; Santa Cruz Biotechnology, Santa Cruz, USA; sc-47724). Subsequently, secondary antibodies were blotted for the detection of corresponding bands by using a ChemiDoc™ Imaging System (Bio-Rad, USA). The quantization of LC3B protein abundances was performed by normalizing the lipidated isoform of the protein (LC3B-II, the lower band in the western blot) against GAPDH, and each band was imaged with Image J software (NIH). For each group, the GC analyses were repeated three times, whereas the analyses for the oocytes and CCs were performed one time, considering that each sample was representative of 100 pooled oocytes or CCs harvested from 100 cumulus-oocyte complexes.

2.5.2. Detection of LC3B protein in GCs, CCs, and oocytes by immunofluorescence

Immunofluorescence analyses were performed on the GCs, CCs, and oocytes and groups to confirm LC3B protein presence and evaluate subcellular localization. To allow cell adhesion, freshly collected GCs and CCs were re-suspended in culture medium (alpha-MEM, Gibco, NY, USA, supplemented with 10% fetal calf serum and 1% penicillin/streptomycin solution), seeded at concentration of 5×10^4 cells/mL on sterile glass coverslips, and incubated for 12–14 h at 38.5 °C in a humidified atmosphere of 5% CO_2 in air. For positive controls (rapamycin-treated cells), 1 μM rapamycin (Abcam, Cambridge, UK; ab120224) was added to cells and incubated for 1 h to chemically induce autophagy. The cells were subsequently washed in PBS, fixed in 4% paraformaldehyde and processed for immunofluorescence analyses. Briefly, after permeabilization and blocking in 10% normal goat serum, GCs, CCs, and oocytes were immunolabelled with rabbit polyclonal primary antibody against LC3B (1:100; Abcam, Cambridge, UK; ab48394), and goat anti-rabbit secondary antibody conjugated to Alexa Fluor 488 Plus (1:800; Thermo Fisher Scientific, Waltham, MA, USA; A32731); each incubation was for 1 h at RT. Nuclei were counter-stained with Hoechst 33342 (1 μg/mL). Negative controls omitted the primary antibody.

At the end of the protocol, the coverslips containing the adherent cells and the oocytes were mounted on glass slides using ProLong antifade reagent (Thermo Fischer Scientific) and observed using a Nikon laser scanning confocal microscope. In immunostaining, dot- and ring-shaped LC3 signals are considered representative of LC3-II protein that is on the autophagosome membrane. This fluorescence pattern in cells, therefore, indicates activated autophagy processes are occurring and is commonly described as “punctate fluorescence”, as it refers to the presence of fluorescent “puncta” or dots (Serke et al., 2009; Choi et al., 2010; Lee et al., 2017). Thus, the percentage of autophagic cells was calculated based on the cells having this fluorescence pattern (LC3-II-positive cells/total cells). For each group, three independent analyses were conducted, and at least 200 cells and 10 oocytes were examined each time.

2.6. Confocal microscopy analysis

The acquisition of fluorescence images was performed using a 60 X oil-immersion objective utilizing a laser scanning confocal microscope (Nikon A1r, Nikon Instruments, Amsterdam, the Netherlands). A 488-nm line excitation of an air-cooled 100 mW argon laser (Spectra Physics) was used; the emitted fluorescence was detected through the combination of the appropriate AG2 filter set with a high pass at 561 nm. Images were captured using the program NIS ELEMENTS 4.40 (Nikon Instruments, Amsterdam, the Netherlands) in sections of 1024 pixels. Scale bars to indicate magnification are provided in the figures of this manuscript.

2.7. Statistical analysis

The percentages of LC3B-II-positive, annexin V-positive and TUNEL-positive cells were reported as the mean ± standard deviation (SD) of at least three independent experiments. The D'Agostino-Pearson omnibus test was performed as a normality test. The data were considered normal, so the statistical analysis was performed using an one-way analysis of variance (ANOVA). Levene’s test was used for assessing homogeneity of variance. Differences with $P < 0.05$ were considered to be statistically significant.

3. Results

3.1. Annexin V-FITC/PI assay in GCs, CCs, and oocytes

The data for incidence of early apoptosis in GCs recovered from healthy and atretic follicles are depicted in the cytofluorimetric analysis plot (Fig. 1A). During the process of follicular atresia there is a progressive increase in the number of early apoptotic cells (PI-/annexin V+, lower right quadrant). In particular, the percentages changed ($P < 0.05$) from 3.2 ± 2.5% in the healthy group to

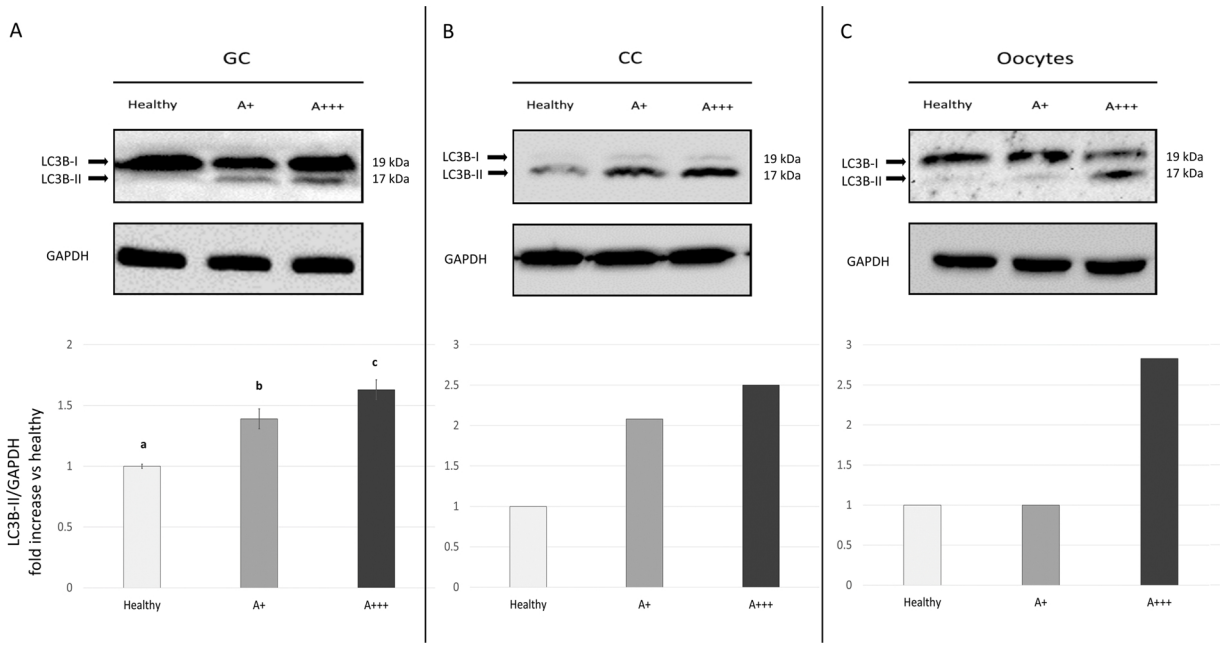

Fig. 2. Western blot analyses of LC3B protein abundance in granulosa cells (GCs), cumulus cells (CCs), and oocytes of sows collected from healthy and atretic antral follicles. Representative immunoblots (up): analyses were conducted with an anti-LC3B antibody and two forms were detected, LC3-I (cytosolic) and LC3-II (autophagosome-membrane bound), as two bands at 19 and 17 kDa (arrows); GAPDH protein was used as a loading control; Densitometric quantifications of LC3B protein abundance (down): the graphs depict the fold increase as compared with the abundance of LC3B-II/GAPDH; In GCs (A), analyses were performed in triplicate; Analyses of oocytes and CCs were performed one time, considering that each sample was representative of 100 pooled oocytes or CCs collected from 100 cumulus-oocyte complexes.

26.5 ± 5.1% and 51.4 ± 1.6% in the ATR + and ATR + + + groups, respectively (Fig. 1B).

Interestingly, the results from the confocal microscopy analyses conducted on CCs and oocytes indicated there were differences compared with the GCs. Here, the annexin V-positive cells (Fig. 1 C2 and C4) were detected as a very small percentage in both cell types, regardless of whether these cells were derived from healthy or atretic follicles (apoptotic CC: healthy 9.1 ± 2.4%; ATR + 12.2 ± 3.8%; ATR + + + 10.0 ± 2.0%; apoptotic oocytes: healthy 4.1 ± 1.5%; ATR + 3.1 ± 1.0%; ATR + + + 5.0 ± 2.1%. $P > 0.05$) (Fig. 1B).

3.2. TUNEL assay in healthy and atretic GCs, CCs, and oocytes

The results from flow-cytometric analysis of GCs from healthy and atretic follicles indicated there was a greater amount of DNA fragmentation (TUNEL-positive cells) for both the ATR+ (46.4 ± 1.3%) and ATR + + + (49.8 ± 5.7%) groups compared with the healthy group (9.4 ± 4.3%, $P < 0.01$; Supplementary Fig. 2 A and C).

In contrast, the results of the TUNEL assay performed on CCs and oocytes indicated that, with the exception of positive control (DNase-treated oocytes), which had a nuclear green fluorescence, almost none of the CCs and oocytes had DNA fragmentation and were thus TUNEL-negative (see supplementary Fig. 2B), regardless of whether these cells were derived from healthy or atretic follicles (apoptotic CCs: healthy 10.7 ± 2.5%, ATR + 16.8 ± 4.0%, ATR + + + 12.3 ± 3.7%; apoptotic oocytes: healthy 2.0 ± 1.5%, ATR + 1.5 ± 1.7%, ATR + + + 2.5 ± 2.3%; $P > 0.05$) (Supplementary Fig. II).

3.3. Western blotting analysis of LC3B protein abundance in GCs, CCs, and oocytes

The abundances of LC3B-II were examined using western blotting in healthy GCs and in both of the different type of atretic GCs. As depicted in Fig. 2, there were two bands on the blots, at approximately 19 and 17 kDa, corresponding to the cytosolic and lipidated isoforms of LC3B, respectively, which are typically detected when autophagy is activated in cells. This finding confirmed that the primary antibody to LC3B used in this research was valid for use in assessments of pig cells, and it also indicated that the normalized abundances of LC3B-II were greater in the ATR + and ATR + + + groups (1.39 and 1.63-fold, respectively), compared to the healthy group ($P < 0.05$) (Fig. 2A). This indicates that autophagy was progressively activated in GCs during follicular atresia at the antral follicle stage.

Concerning the abundance of LC3B-II in CCs, the results were similar to those for GCs. There was detection of increased values of LC3B-II/GAPDH in both the ATR + and ATR+ + + CC groups (2.08 and 2.50-fold, respectively) compared to healthy CCs (Fig. 2B). Furthermore, there was a greater abundance of the autophagic marker in ATR+ + + oocytes as compared with healthy oocytes (2.83-fold greater) (Fig. 2C).

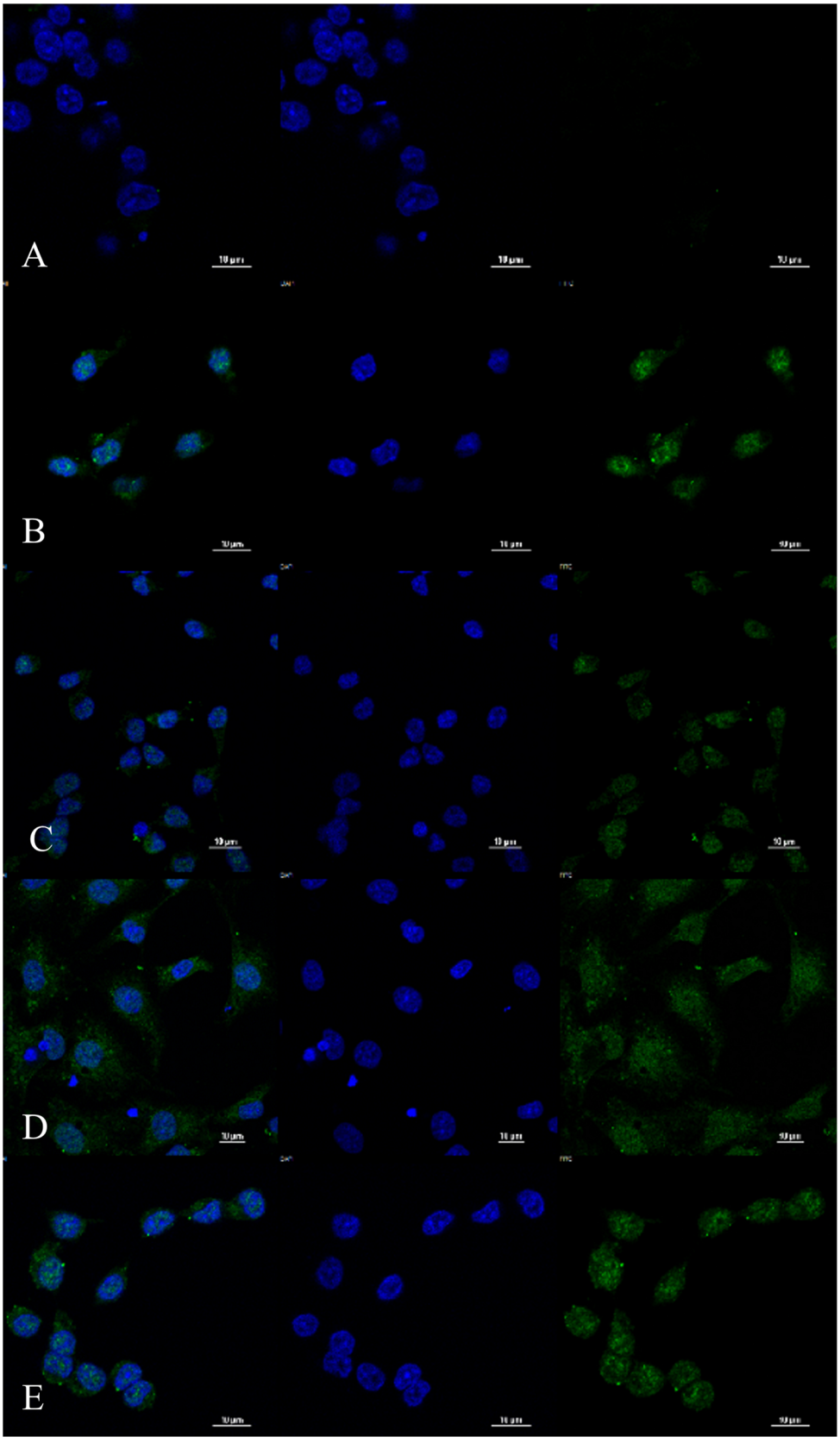

(caption on next page)

Fig. 3. Immunofluorescence analysis of LC3B protein in granulosa cells (GCs) of healthy and atretic follicles of sows.
Representative confocal microscopy images of GCs of sows immunostained with primary LC3B antibody, secondary Alexa Fluor Plus 488 antibody (green fluorescence), and counterstained with Hoechst 33342 (blue fluorescence); All groups had the LC3B protein, but a different abundance of LC3B-II-positive cells (undergoing induced autophagy) was detected; Most early (D) and advanced (E) atretic cells, as well as rapamycin-treated cells (positive control, B), had the typical punctate fluorescence pattern that is associated with LC3B-II protein in the autophagosome membrane; In contrast, most healthy GCs (C) had a diffused fluorescence, without fluorescent puncta; (A) Negative control without primary antibody; scale bars: 10 μm

3.4. Detection of LC3B protein by immunofluorescence

The LC3B protein was present in all GC groups with the exception of the negative control. When there was consideration of only the cells having the punctate pattern of fluorescence, the percentages of LC3B-II-positive cells changed depending on whether these were from healthy or atretic follicles, as depicted in Fig. 3. In fact, the majority of atretic GCs, both at early and late stages of atresia, were positive (73.0 ± 13.6% and 83.6 ± 6.2%, respectively), and there was a similar situation in rapamycin-treated GCs, where autophagy was chemically-induced (positive control, 78.4 ± 11.9%). In contrast, the percentage of cells having punctate fluorescence was lower in healthy GCs (37.7 ± 7.0%) ($P < 0.05$) compared with all other groups, and most of these cells had a diffused fluorescence pattern (Fig. 3C).

There were similar results from the immunofluorescence analysis conducted with CCs (Fig. 4), with all cells containing the LC3B protein, and the majority of CCs having a punctate fluorescence in the atretic groups, as well as in the positive control. In particular, the percentage of LC3B-II-positive cells was greater in the ATR+ (68.8 ± 6.0%) and ATR + + + (67.9 ± 8.7%) groups, as well as in the rapamycin-treated group (84.0 ± 3.1%) compared to healthy CCs (37.6 ± 12.5%) ($P < 0.05$).

Furthermore, there was a distinct punctate pattern of fluorescence detected in oocytes (Fig. 5), with a markedly greater percentage of positive cells in the rapamycin-treated (65.4 ± 7.4%) and atretic groups (ATR + 60.9 ± 5.9%, ATR + + + 58.8 ± 7.3%) compared with healthy cells (25.2 ± 3.3%) ($P < 0.05$).

4. Discussion

In mammalian ovaries, a balance between cell proliferation and cell death is maintained in healthy follicles, and any imbalance of the two processes can lead to atresia of the follicle. Although follicular atresia affects all stages of folliculogenesis, in sows the greatest incidence of follicular degeneration occurs during the antral stage (Clark et al., 1982; Morbeck et al., 1992), involving the extensive death of GCs (Morita and Tilly, 1999; Escobar Sánchez et al., 2012; Spanel-Borowski, 2012). It is accepted that both apoptosis and autophagy, two types of PCD, can have a role in follicular atresia, but the connection between the two processes remains to be elucidated. Species-specific differences exist, and the available data are incomplete and sometimes conflicting (Eisenberg-Lerner et al., 2009; Yadav et al., 2018). Furthermore, in CCs and oocytes of pigs, the process of autophagy has never been evaluated *in vivo* in relation to atresia during the antral stage of follicular development.

Results with western blotting in the present study indicate the LC3B protein is present in porcine GCs, and that the abundance of its autophagosome-associated form is greater in GCs of atretic follicles compared to healthy follicles. These results are consistent with those in previous studies in rodents (Choi et al., 2010) and humans (Duerrschmidt et al., 2006; Serke et al., 2009; Vilser et al., 2010). Furthermore, in the present study the increase of LC3B-II abundance in atretic GCs is progressive during the process of atresia.

The relatively greater abundance of LC3B-II in atretic GCs in the present study was confirmed by results with immunofluorescence analyses. Although moderate to intensive immunostaining of LC3B protein was detected in both healthy and atretic GCs, when the LC3B-II form of the protein was evaluated, there was a different incidence of positive cells amongst the experimental groups. Additionally, consistent with results from the western blotting analysis in the present study, the percentage of cells having a punctate pattern of fluorescence (indicative of induced autophagy) increased progressively from the early to the advanced stage of atresia.

Thus, the results of the present study indicate, for the first time, that in sow ovaries the induction of autophagy in GCs is correlated to the antral follicle selection that takes place during pre-ovulatory maturation. The results of the same analyses conducted on CCs indicated there was a similar occurrence to that of GCs regarding the induction of autophagy. Importantly, results from both analyses indicate, for the first time, the relatively greater abundance of LC3B-II in early and advanced atretic CCs, which progressively increased compared to healthy cells. Furthermore, there was a greater abundance of LC3B-II protein in advanced atretic oocytes, indicating that during follicle degeneration, autophagy is activated in gametes as well.

The combined results from evaluation of CCs and oocytes of sows also highlights the presence of species-specific differences because in rats, induced autophagy has been documented in GCs but not in CCs and oocytes during antral follicle atresia (Choi et al., 2010; Meng et al., 2018). This finding may not be surprising considering there is a difference between rodents and pigs when the site of apoptosis is evaluated. As previously reported by Manabe et al. (1997, 2004) and confirmed by the present research, in pigs, the GCs represent almost the exclusive target of apoptosis during the process of follicular atresia at the antral stage, unlike in rodents where apoptosis occurs in GCs as well as in CCs and oocytes. In the present study, results from the annexin V and TUNEL analyses indicate there are very few apoptotic gametes and surrounding cells collected from early and advanced atretic follicles, whereas apoptosis was detected in a large percentage of atretic GCs. Even at the early stage of atresia, there was a markedly greater percentage of GCs with membrane changes (annexin V-positive cells) compared to healthy cells. When the process of atresia is in an advanced stage, approximately half of the cell population has both PS externalization and DNA fragmentation simultaneously, thus, indicating

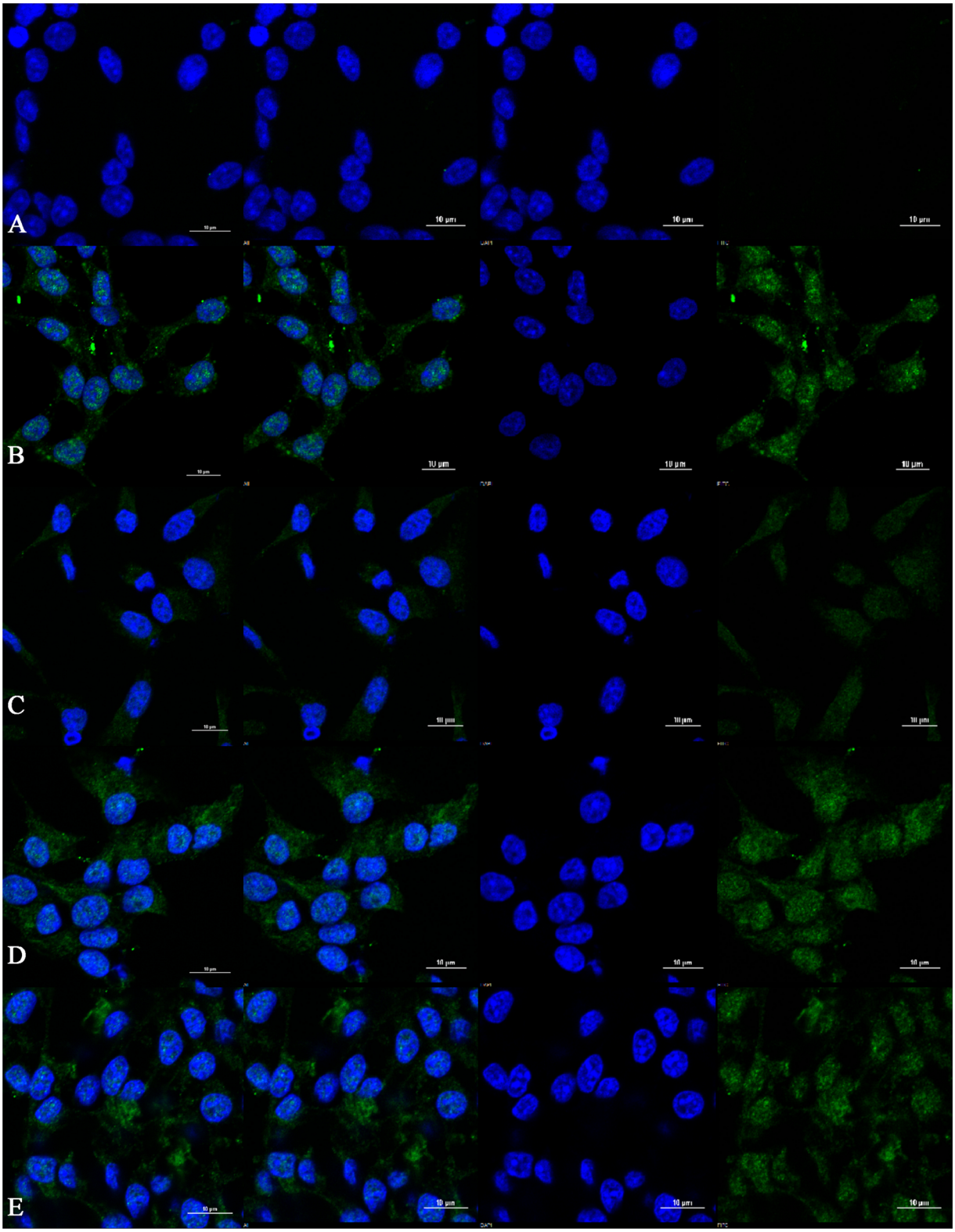

(caption on next page)

Fig. 4. Immunofluorescence analysis of LC3B protein in cumulus cells (CCs) of healthy and atretic follicles of sows.
Representative confocal microscopy images of CCs of sows immunostained with primary LC3B antibody, secondary Alexa Fluor 488 Plus antibody (green fluorescence), and counterstained with Hoechst 33342 (blue fluorescence); Autophagic cells with green fluorescence puncta were evident in the majority of both atretic groups (D, early atretic; E, advanced atretic) and in the positive control (B, rapamycin-treated cells); In contrast, most healthy cells (C) had a diffuse fluorescence without a punctate pattern; no fluorescence signal was detected in the negative control (A) where primary antibody was omitted; scale bars: 10 μm

that early and late processes of apoptosis are activated in parallel in GCs of pigs during antral follicle atresia.

To our knowledge, the present research documents, for the first time, the site of autophagy and the relationship between autophagy and apoptosis during the physiological process of atresia in antral follicles of sow ovaries, highlighting the differences between pigs and rodents.There may be various reasons for these inconsistencies in the follicular atresia process among species. Follicular atresia is strictly dependent on local ovarian factors (Tsafriri and Braw, 1984), and apoptosis and autophagy that occurs in follicular cells, as well as in the part of the follicle where there is induction of these processes, may vary depending on the stage of follicular development and the stage of sexual immaturity or maturity. These factors influence the capacity for studying the involvement of these PCD mechanisms (Manabe et al., 2004). Differently from Choi et al. (2014), who used immature rats to analyse LC3 abundance in the GCs of healthy or atretic antral follicles, sow ovaries were used in the present study, which have a complete estrous cycle rather than the truncated reproductive cycle that prevails in rats. Furthermore, with sow ovaries it is easier to precisely surgically manipulate and isolate each component of the follicle using a surgical microscope so that there can be an accurate study of various follicular components.

Regarding the differing involvement of autophagy in CCs and oocytes of pigs and rats, it could be hypothesized that there is a species-specific function for this process. There have been a number of reports indicating autophagy and apoptosis can have opposing functions by either synergistic (Kabeya et al., 2000, 2004; Choi et al., 2010) or antagonistic actions to prevent apoptotic cell death (Xue et al., 2001; Kanzawa et al., 2003). In fact, autophagy is known to be activated in cells as a survival mechanism when there are specific adverse conditions, such as starvation (Ferraro and Cecconi, 2017; Huang et al., 2015). There is a similar occurrence in large pig follicles during atresia due to a marked reduction of vascularization (Cran et al., 1983; Greenwald and Terranova, 1988; Martelli et al., 2006). The consequent GC death may deprive the CCs and oocyte of nutrients and regulatory molecules, and this constituent milieu within the follicle may lead to induction of autophagy in these cells as a cytoprotective mechanism. This hypothesis is consistent with the absence of apoptosis in the majority of CCs and oocytes at the time of autophagy. A pro-survival function during autophagy in the cumulus-oocyte complex could be important in a species such as the pig that is characterized by a long-lasting folliculogenesis process compared to rodents, allowing the supply of the necessary trophic and regulatory molecules that could preserve the viability and function of CC for a longer period of time and, consequently, preserve the oocyte. It is well known that coupling between the CCs and the gametes is important throughout folliculogenesis and oocyte maturation and that during the period before ovulation, the pig oocyte undergoes dramatic changes (Eppig, 1985; Kidder and Mhawi, 2002). During this time, therefore, a function of the autophagy process in the cytosolic growth and maturation of the oocyte can be inferred by the degradation and recycling of gap junctions or imported substances *via* gap junctions, as occurs in other cell types (Carette et al., 2015; Sun et al., 2015). Further studies are necessary to investigate this hypothesis.

5. Conclusions

In pig ovaries, there is a greater LC3B-II abundance in GCs, CCs, and oocytes of antral follicles destined to degenerate, indicating induced autophagy in all of these cell types. Species-specific differences exist regarding the association between autophagy and apoptosis during antral follicle maturation *in vivo*. In particular, in pigs (as in rodents), the induced autophagy in GCs could have a cooperative function with apoptosis in directing the follicle towards atresia. Only in CCs and oocytes of pigs does the induction of autophagy have an opposing function to apoptosis, functioning as a cytoprotective mechanism to maintain the viability and function of the gamete and the coupled cells for a longer period of time.

Funding

This research did not receive any specific grant from funding agencies in the public, commercial, or not-for-profit sectors.

Color artwork

The authors declare that color should be used for any figures in print.

Declaration of Competing Interest

The authors declared that they have no conflicts of interest regarding this work.

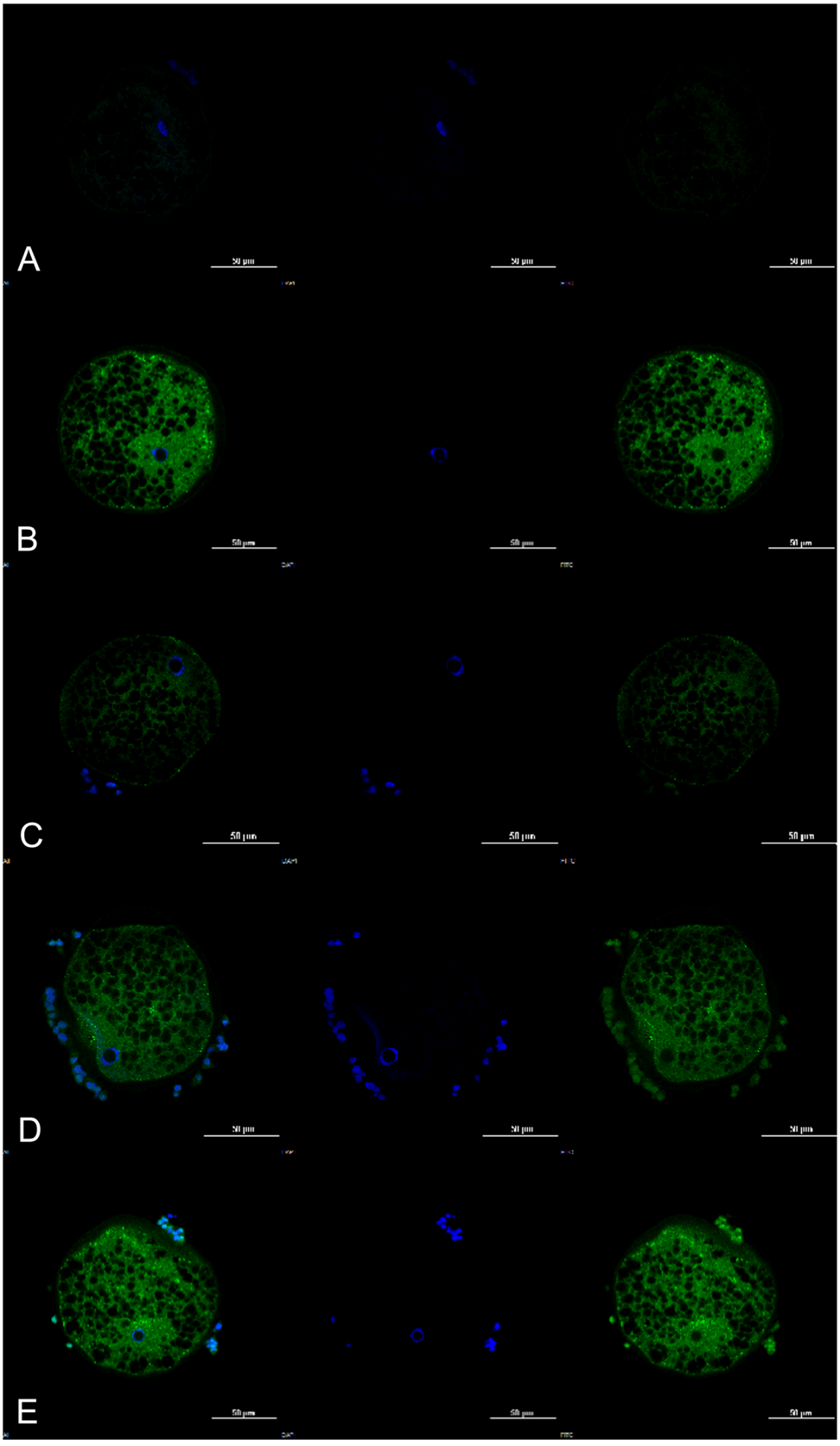

(caption on next page)

Fig. 5. Immunofluorescence analysis of LC3B protein in oocytes collected from healthy and atretic antral follicles of sows.
Oocytes were immunostained with a primary LC3B antibody, secondary Alexa Fluor Plus 488 antibody (green fluorescence), counterstained with Hoechst 33342 (blue fluorescence), and were visualized using a confocal microscope; Representative images of negative control (A), rapamycin-treated (B), healthy (C), early atretic (D), and advanced atretic (E) oocytes; In both atretic groups, and in rapamycin-treated oocytes where autophagy was chemically induced, green fluorescence puncta were evident in the cytoplasm; This was different from the healthy oocytes that only had a diffused fluorescence; scale bars: 50 μm

Acknowledgements

The authors thank Maria Tufolo and Roberto Piccirilli for technical assistance and Dr. Nicola Bernabò who provided help for the statistical analysis of the data.

Appendix A. Supplementary data

Supplementary material related to this article can be found, in the online version, at doi:10.1016/j.anireprosci.2019.106225.

References

Anchordoquy, J.P., Anchordoquy, J.M., Picco, S.J., Sirini, M.A., Errecalde, A.L., Furnus, C.C., 2014. Influence of manganese on apoptosis and glutathione content of cumulus cells during in vitro maturation in bovine oocytes. Cell Biol. Int. 38, 246–253. https://doi.org/10.1002/cbin.10195.

Byskov, A.G., 1974. Cell kinetic studies of follicular atresia in the mouse ovary. J. Reprod. Fertil. 37, 277–285.

Carette, D., Gilleron, J., Denizot, J.P., Grant, K., Pointis, G., Segretain, D., 2015. New cellular mechanisms of gap junction degradation and recycling. Biol. Cell 107, 218–231. https://doi.org/10.1111/boc.201400048.

Choi, J., Jo, M., Lee, E., Choi, D., 2014. AKT is involved in granulosa cell autophagy regulation via mTOR signaling during rat follicular development and atresia. Reproduction 147, 73–80. https://doi.org/10.1530/REP-13-0386.

Choi, J.Y., Jo, M.W., Lee, E.Y., Yoon, B.K., Choi, D.S., 2010. The role of autophagy in follicular development and atresia in rat granulosa cells. Fertil. Steril. 93, 2532–2537. https://doi.org/10.1016/j.fertnstert.2009.11.021.

Clark, J.R., Brazier, S.G., Wiginton, L.M., Stevenson, G.R., Tribble, L.F., 1982. Time of ovarian follicle selection during the porcine estrous cycle. Theriogenology 18, 697–709. https://doi.org/10.1016/0093-691X(82)90035-8.

Cran, D.G., Osborn, J.C., Rushton, D., 1983. Thecal vasculature and oocyte maturation during follicular atresia in the sheep and pig. Reprod. Nutr. Dev. 23, 285–292.

Duerrschmidt, N., Zabirnyk, O., Nowicki, M., Ricken, A., Hmeidan, F.A., Blumenauer, V., Borlak, J., Spanel-Borowski, K., 2006. Lectin-like oxidized low-density lipoprotein receptor-1-mediated autophagy in human granulosa cells as an alternative of programmed cell death. Endocrinology 147, 3851–3860. https://doi.org/10.1210/en.2006-0088.

Eisenberg-Lerner, A., Bialik, S., Simon, H.U., Kimchi, A., 2009. Life and death partners: apoptosis, autophagy and the cross-talk between them. Cell Death Differ. 16, 966–975.

Eppig, J.J., 1985. Oocyte-somatic cell interactions during oocyte growth and maturation in the mammal. In: In: Browder, L.W. (Ed.), Oogenesis. Developmental Biology (A Comprehensive Synthesis), vol. 1 Springer, Boston, MA. https://doi.org/10.1007/978-1-4615-6814-8_7.

Escobar, M.L., Echeverría, O.M., Vázquez-Nin, G.H., 2013. Role of Autophagy in the Ovary Cell Death in Mammals. https://doi.org/10.5772/54777.

Escobar Sánchez, M.L., Echeverría Martínez, O.M., Vázquez-Nin, G.H., 2012. Immunohistochemical and ultrastructural visualization of different routes of oocyte elimination in adult rats. Eur. J. Histochem. 56 (2), e17. https://doi.org/10.4081/ejh.2012.17.

Ferraro, E., Cecconi, F., 2017. Autophagic and apoptotic response to stress signals in mammalian cells. Arch. Biochem. Biophys. 462, 210–219. https://doi.org/10.1016/j.abb.2007.02.006.

Gao, H., Lin, L., Haq, I.U., Zeng, S., 2016. Inhibition of NF-kB promotes autophagy via JNK signaling pathway in porcine granulosa cells. Biochem. Biophys. Res. Commun. 1–6 https:// doi.org/10.1016/j.bbrc.2016.03.101.

Gioia, L., Barboni, B., Turriani, M., Capacchietti, G., Pistilli, M.G., Berardinelli, P., Mattioli, M., 2005. The capability of reprogramming the male chromatin after fertilization is dependent on the quality of oocyte maturation. Reproduction 130, 29–39 https:// doi.org/10.1530/rep.1.00550.

Greenwald, G.S., Terranova, P.F., 1988. In: Knobil, E., Neilet Al, J. (Eds.), Follicular Selection and Its Control, in: The Physiology of Reproduction. Raven Press, Ltd., New York.

Hale, B.J., Hager, C.L., Seibert, J.T., Selsby, J.T., Baumgard, L.H., Keating, A.F., Ross, J.W., 2017. Heat stress induces autophagy in pig ovaries during follicular development. Biol. Reprod. 97, 426–437 https://doi: 10.1093/biolre/iox097.

Huang, R., Xu, Y., Wan, W., Shou, X., Qian, J., You, Z., Liu, B., Chang, C., Zhou, T., Lippincott-Schwartz, J., Liu, W., 2015. Deacetylation of nuclear LC3 drives autophagy initiation under starvation. Mol. Cell 57, 456–466. https://doi.org/10.1016/j.molcel.2014.12.013.

Kabeya, Y., Mizushima, N., Ueno, T., Yamamoto, A., Kirisako, T., Noda, T., Kominami, E., Ohsumi, Y., Yoshimori, T., 2000. LC3, a mammalian homologue of yeast Apg8p, is localized in autophagosome membranes after processing. EMBO J. 19, 5720–5728.

Kabeya, Y., Mizushima, N., Yamamoto, A., Ohsitani-Okamoto, S., Oshumi, Y., Yoshimori, T., 2004. LC3, GABARAP and GATE16 localize to autophagosomal membrane depending on form-II formation. J. Cell. Sci. 117, 2805–2812.

Kaipia, A., Hsueh, A.J.W., 1997. Regulation of ovarian follicle atresia. Ann. Rev. Physiol. 59, 349–363.

Kanzawa, T., Kondo, Y., Ito, H., Kondo, S., Germano, I., 2003. Induction of autophagic cell death in malignant glioma cells by arsenic trioxide. Cancer Res. 63, 2103–2108.

Kidder, G.M., Mhawi, A.A., 2002. Gap junctions and ovarian folliculogenesis. Reproduction 123, 613–620.

Kim, S.H., Hwang, S.Y., Min, K.S., Yoon, J.T., 2013. Molecular cloning and expression analysis of porcine MAPLC3A in the granulosa cells of nornal and miniature pig. Reprod. Biol. Endocrinol. 11, 8 https://doi: 10.1186/1477-7827-11-8.

Klionsky, D.J., Schulman, B.A., 2014. Dynamic regulation of macroautophagy by distinctive ubiquitin-like proteins. Nat. Struct. Mol. Biol. 21, 336–345 https://doi: 10.1038/nsmb.2787.

Lee, S., Kim, D.H., Im, G.S., Ock, S.A., Ullah, I., Hur, T.Y., 2017. Localization of autophagosomes in porcine follicular cumulus-oocyte complex. J. Emb. Trans. 32, 105–109.

Lin, P., Rui, R., 2010. Effects of follicular size and FSH on granulosa cell apoptosis and atresia in porcine antral follicles. Mol. Reprod. Dev. 77, 670–678. https://doi.org/10.1002/mrd.21202.

Manabe, N., Goto, Y., Matsuda-Minehata, F., Inoue, N., Maeda, A., Sakamaki, K., Miyano, T., 2004. Regulation mechanism of selective atresia in porcine follicles: regulation of granulosa cell apoptosis during atresia. J. Reprod. Dev. 50, 493–514. https://doi.org/10.1262/jrd.50.493.

Manabe, N., Imai, Y., Myoumoto, A., Kimura, Y., Sugimoto, M., Okamura, Y., Fukumoto, M., Sakamaki, K., Miyamoto, H., 1997. Apoptosis occurs in granulosa cells but not cumulus cells in the atretic graafian follicles in multiparous pig ovaries. Acta. Histochem. Cytochem. 30, 85–92. https://doi.org/10.1267/ahc.30.85.

Martelli, A., Berardinelli, P., Russo, V., Mauro, A., Bernabo, N., Gioia, L., Mattioli, M., Barboni, B., 2006. Spatio-temporal analysis of vascular endothelial growth factor

expression and blood vessel remodelling in pig ovarian follicles during the periovulatory period. J. Mol. Endocrinol. 36, 107–119.
Matsuda, F., Inoue, N., Manabe, N., Ohkura, S., 2012. Follicular growth and atresia in mammalian ovaries: regulation by survival and death of granulosa cells. J. Reprod. Dev. 58, 44–50. https://doi.org/10.1262/jrd.2011-012.
Mattioli, M., Barboni, B., Gioia, L., Loi, P., 2003. Cold-induced calcium elevation triggers DNA fragmentation in immature pig oocytes. Mol. Reprod. Dev. 65, 289–297 https:// doi.org/10.1002/mrd.10275.
Meineke, B., Meineke-Tillmann, S., Gips, H., 1982. Experimentelle untersuchungen zur steroidsekretionintakter und atretischer follikel in vitro. Berl. Munch.Tierarztl. Wochenschr. 95, 107–111.
Meng, L., Jan, S.Z., Hamer, G., van Pelt, A.M., van der Stelt, I., Keijer, J., Teerds, K.J., 2018. Preantral follicular atresia occurs mainly through autophagy, while antral follicles degenerate mostly through apoptosis. Biol. Reprod. 99, 853–863 https://doi: 10.1093/biolre/ioy116.
Mohn, C., Long, K., Mutneja, M., Ma, J., 2015. Detection of End-stage apoptosis by ApopTag®TUNEL technique. In: In: Mor, G., Alvero, A. (Eds.), Apoptosis and Cancer, Methods in Molecular Biology (Methods and Protocols)., vol. 1219. Humana Press, New York, pp. 43–56. https://doi.org/10.1007/978-1-4939-1661-0_5.
Morais, R.D.V.S., Thomé, R.G., Lemos, F.S., Bazzoli, N., Rizzo, E., 2012. Autophagy and apoptosis interplay during follicular atresia in fish ovary: a morphological and immunocytochemical study. Cell Tissue Res. 347, 467–478. https://doi.org/10.1007/s00441-012-1327-6.
Morbeck, D., Esbenshade, K., Flowers, W., Britt, J., 1992. Kinetics of follicle growth in the prepubertal gilt. Biol. Reprod. 47, 485–491. https://doi.org/10.1095/biolreprod47.3.485.
Morita, Y., Tilly, J.L., 1999. Oocyte apoptosis: like sand through an hourglass. Dev. Biol. 213, 1–17. https://doi.org/10.1006/dbio.1999.9344.
Ortiz, R., Echeverría, O.M., Salgado, R., Escobar, M.L., Vázquez-Nin, G.H., 2006. Fine structural and cytochemical analysis of the processes of cell death of oocytes in atretic follicles in new born and prepubertal rats. Apoptosis 11, 25–37. https://doi.org/10.1007/s10495-005-3347-0.
Ryter, S.W., Mizumura, K., Choi, A.M.K., 2014. The impact of autophagy on cell death modalities. Int. J. Cell Biol. https://doi.org/10.1155/2014/502676.
Serke, H., Vilser, C., Nowicki, M., Hmeidan, F.A., Blumenauer, V., Hummitzsch, K., Lösche, A., Spanel-Borowski, K., 2009. Granulosa cell subtypes respond by autophagy or cell death to oxLDL-dependent activation of the oxidized lipoprotein receptor 1 and toll-like 4 receptor. Autophagy 5, 991–1003.
Spanel-Borowski, K., 2012. Follicle stages and follicular atresia. Atlas of the Mammalian Ovary. Springer, Berlin Heidelberg, Berlin, Heidelberg, pp. 9–22. https://doi.org/10.1007/978-3-642-30535-1_2.
Sun, L.Q., Gao, J.L., Cui, Y., Zhao, M.M., Jing, X.B., Li, R., Tian, Y.X., Cui, J.Z., Wu, Z.X., 2015. Neuronic autophagy contributes to p-connexin 43 degradation in hippocampal astrocytes following traumatic brain injury in rats. Mol. Med. Rep. 11, 4419–4423 https://doi: 10.3892/mmr.2015.3264.
Tsafriri, A., Braw, R.H., 1984. Experimental approach to atresia in mammals. Oxf. Rev. Reprod. Biol. 6, 226–265.
Vermes, I., Haanen, C., Steffens-Nakken, H., Reuteligsperger, C., 1995. A novel assay for apoptosis flow-cytometric detection of phosphatidylserine expression on early apoptotic cell using fluorescein labeled Annexin V. J. Immunol. Methods 184, 39–51 https:// doi.org/10.1016/0022-1759(95)00072-i.
Vilser, C., Hueller, H., Nowicki, M., Hmeidan, F.A., Blumenauer, V., Spanel-Borowski, K., 2010. The variable expression of lectin-like oxidized low-density lipoprotein receptor (LOX-1) and signs of autophagy and apoptosis in freshly harvested human granulosa cells depend on gonadotropin dose, age, and body weight. Fertil. Steril. 93, 2706–2715. https://doi.org/10.1016/j.fertnstert.2009.02.038.
Wang, W., Tang, Y., Ni, L., Jongwutiwes, T., Liu, H.-C., Rosenwaks, Z., 2012. A modified protocol for in vitro maturation of mouse oocytes from secondary preantral follicles. Adv. Biosci. Biotechnol. 3, 57–74. https://doi.org/10.4236/abb.2012.31010.
Xue, L., Fletcher, G.C., Tolkovsky, A.M., 2001. Mitochondria are selectively eliminated from eukaryotic cells after blockade of caspases during apoptosis. Curr. Biol. 11, 361–365. https://doi.org/10.1016/S0960-9822(01)00100-2.
Yadav, P.K., Tiwari, M., Gupta, A., Sharma, A., Prasad, S., Pandey, A.N., Chaube, S.K., 2018. Germ cell depletion from mammalian ovary: possible involvement of apoptosis and autophagy. J. Biomed. Sci. 25, 36. https://doi.org/10.1186/s12929-018-0438-0.